Predissociation mechanism for the lowest u 1 states of N 2

B. R. Lewis, S. T. Gibson, W. Zhang, H. Lefebvre-Brion, and J.-M. Robbe

Citation: The Journal of Chemical Physics **122**, 144302 (2005); doi: 10.1063/1.1869986
View online: http://dx.doi.org/10.1063/1.1869986
View Table of Contents: http://scitation.aip.org/content/aip/journal/jcp/122/14?ver=pdfcov
Published by the AIP Publishing

Predissociation mechanism for the lowest $^1\Pi_u$ states of N_2

B. R. Lewis, S. T. Gibson, and W. Zhang[a)]
Research School of Physical Sciences and Engineering, The Australian National University, Canberra, Australian Capital Territory 0200, Australia

H. Lefebvre-Brion
Laboratoire de Photophysique Moléculaire, Bâtiment 213, Université de Paris-Sud, 91405 Orsay Cedex, France

J.-M. Robbe
Laboratoire de Physique des Atomes, Lasers, et Molécules, Université de Lille I, UFR de Physique Fondamentale, F-59655 Villeneuve d'Ascq, France

(Received 29 October 2004; accepted 20 January 2005; published online 8 April 2005)

Separate coupled-channel Schrödinger-equation (CSE) models of the interacting $^1\Pi_u$ (b,c,o) and $^3\Pi_u$ (C,C') states of N_2 are combined, through the inclusion of spin-orbit interactions, to produce a five-channel CSE model of the N_2 predissociation. Comparison of the model calculations with an experimental database, consisting principally of detailed new measurements of the vibrational and isotopic dependence of the $^1\Pi_u$ linewidths and lifetimes, provides convincing evidence that the predissociation of the lowest $^1\Pi_u$ levels in N_2 is primarily an *indirect* process, involving spin-orbit coupling between the $b\,^1\Pi_u$- and $C\,^3\Pi_u$-state levels, the latter levels themselves heavily predissociated electrostatically by the $C'\,^3\Pi_u$ continuum. The well-known large width of the $b(v=3)$ level in $^{14}N_2$ is caused by an accidental degeneracy with $C(v=9)$. This CSE model provides the first quantitative explanation of the predissociation mechanism for the dipole-accessible $^1\Pi_u$ states of N_2, and is thus likely to prove useful in the construction of realistic radiative-transfer and photochemical models for nitrogen-rich planetary atmospheres. © *2005 American Institute of Physics*. [DOI: 10.1063/1.1869986]

I. INTRODUCTION

The upper states of the first electric-dipole-allowed transitions of the nitrogen molecule, i.e., the $^1\Pi_u$ and $^1\Sigma_u^+$ states in the $\gtrsim$101 000 cm^{-1} region, were very difficult to interpret prior to the simultaneous works of three authors,[1–3] who showed that the chaotic pattern of energy levels for each symmetry could only be explained within a framework of strong Rydberg-valence interaction. Carroll and Collins[3] also noted that most of the vibrational levels of the $b\,^1\Pi_u$ valence state were predissociated, with only the $b(v=1,5,6)$ levels giving rise to emission spectra. Considering the importance of the decay mechanisms for the $^1\Pi_u$ states to the elucidation of radiative and photochemical processes in nitrogen-rich planetary atmospheres, it is surprising that these mechanisms have yet to be conclusively established. Certainly, no quantitative model of the N_2 predissociation has yet been developed.

Potential-energy curves for the lowest singlet and triplet Π_u states of N_2, shown schematically in Fig. 1, demonstrate some of the complexity of the electronic structure in this energy region. While most of Fig. 1 is shown in a *diabatic* representation, in which potentials for states of like symmetry are allowed to cross, the $^3\Pi_u$ valence-state manifold is derived from the *ab initio* calculations of Partridge,[4] and is thus in an *adiabatic* representation, including avoided crossings. Hereafter in this work, when discussing the roles of the $C\,^3\Pi_u$ and $C'\,^3\Pi_u$ states, we refer only to the diabatic (crossing) states.

Both Dressler[2] and Carroll and Collins[3] discussed possible predissociation mechanisms for the $^1\Pi_u$ states of N_2,

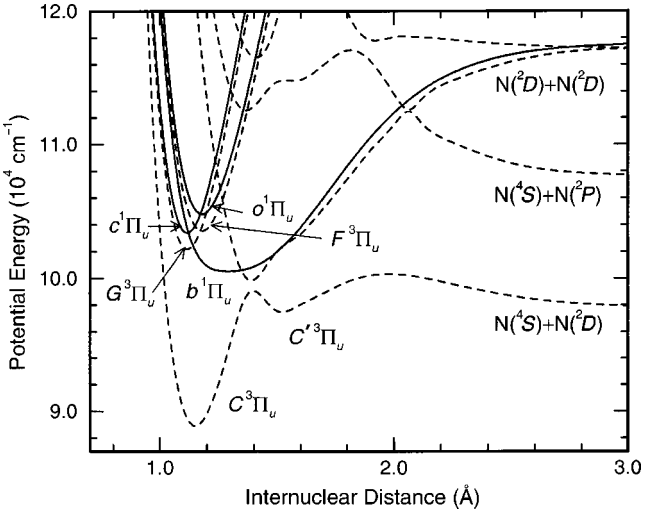

FIG. 1. The lowest-energy $^1\Pi_u$ (solid curves) and $^3\Pi_u$ (dashed curves) potential-energy curves of N_2, referred to the $v=0$, $J=0$ level of the $X\,^1\Sigma_g^+$ ground state (not shown). The $^1\Pi_u$ potentials are taken from the diabatic model of Spelsberg and Meyer (Ref. 19), the $^3\Pi_u$ valence potentials are from spline fits to the *ab initio* calculations of Partridge (Ref. 4), and the Rydberg $F,G\,^3\Pi_u$ potentials are derived by shifting the $o,c\,^1\Pi_u$ potentials in energy to be consistent with the results of Ref. 10. The lowest dissociation limit, N(^4S)+N(^4S) at ~78 710 cm^{-1}, is beyond the scale of the figure.

[a)]Present address: University of Melbourne, Parkville, VIC 3052, Australia.

concluding that the predissociation could not be of the allowed type, since no $^1\Pi_u$, $^1\Sigma_u$, or $^1\Delta_u$ continua, correlating with a low-enough dissociation limit, existed. Through a process of elimination, both authors concluded that the likely *ultimate* predissociation channel was the $C'\,^3\Pi_u$ state, correlating with the $^4S+^2D$ dissociation limit at $\sim$97 940 cm^{-1}. Carroll and Collins[3] suggested a *direct* predissociation of $b\,^1\Pi_u$ by $C'\,^3\Pi_u$, while canvassing possible alternatives. However, Dressler[2] felt that the erratic vibrational dependence of the predissociation favored an *indirect* mechanism, mediated by accidental energy degeneracies between the *b*-state levels and levels of the $C\,^3\Pi_u$ state, which were, in turn, strongly predissociated by the C' continuum. Later, Leoni and Dressler[5] attempted, not very successfully, to model their experimental $^1\Pi_u$ linewidth data assuming direct predissociation by the C' state, but also citing accidental predissociation by the $F\,^3\Pi_u(v=0)$ Rydberg state to explain the large width of $\sim$20 cm^{-1} full width at half maximum (FWHM) that they observed for $b(v=3)$.

An analysis of these different interpretations formed a significant part of the combined experimental and theoretical study of Robbe,[6] who found a much smaller $b(v=3)$ width of $\sim$3 cm^{-1} FWHM, and argued, on theoretical grounds, that the $F(v=0)$ level must occur at a higher energy than supposed by Leoni and Dressler,[5] thus being unavailable to accidentally predissociate $b(v=3)$. Using a combined *ab initio* and coupled-channel Schrödinger-equation (CSE) theoretical treatment, Robbe[6] concluded that the $b(v=3)$ level was accidentally predissociated by $C(v=8)$, a result reported in Ref. 7, but his model, which also included direct spin-orbit predissociation by the C' state, was unable to describe the vibrational pattern of the *b*-state predissociation.

Since the work of Robbe in 1978,[6] there have been many experimental studies of predissociation in N_2, some of which included well-considered discussions of the possible predissociation mechanisms,[8,9] but there have been no successful attempts quantitatively to explain the observed linewidths and lifetimes. However, an important breakthrough occurred in the photofragment-spectroscopic study of van der Kamp *et al.*,[10] who showed unambiguously that the $F(v=0)$ level occurs near 104 500 cm^{-1}, well above the $b(v=3)$ level near 102 860 cm^{-1}, thus supporting the contention of Robbe.[6] This result rules out the *F* state as an indirect channel for the predissociation of the lowest *b*-state levels, in disagreement with the model of Leoni and Dressler.[5]

The aim of the present study is to establish, once and for all, the applicable predissociation mechanism for the lowest $^1\Pi_u$ states of N_2, through the development of a quantitative CSE model which reproduces the experimental database of linewidths and lifetimes. This study is timely, in the sense that extensive new experimental information on the linewidths and lifetimes has recently become available,[11–14] including data on isotopic dependence, which will severely constrain and test any model of the N_2 predissociation. Much of this new data, with which our model results are compared, appear in the preceding companion paper in this issue.[11]

II. COUPLED-CHANNEL MODEL

We employ the coupled-channel Schrödinger-equation technique[15] to treat the $^{1,3}\Pi_u$ states of N_2 and their interactions. A similar application of the CSE technique has been described in detail, e.g., for the case of molecular oxygen, in Ref. 16. Briefly, the diabatic-basis coupled-channel radial Schrödinger equation for the coupled Π_u states is solved numerically to yield the coupled-channel wave function for the excited state, which is then combined with the ground-state radial wave function and appropriate diabatic electronic transition moments, to form the total photodissociation cross section. Transition energies and predissociation linewidths derived from the computed cross section are then compared with experiment iteratively, in order to optimize the CSE-model parameters. Isotopic calculations are performed simply by changing the value of the reduced molecular mass in the CSE model, while rotational calculations are performed by including an appropriate centrifugal term in the Hamiltonian.

A. Electrostatic interactions and spectroscopy

The diabatic $^{1,3}\Pi_u$ electronic states of N_2 are associated primarily with the following molecular-orbital (MO) configurations:

$$c\,^1\Pi_u, G\,^3\Pi_u: \cdots (2\sigma_u)^2(3\sigma_g)(1\pi_u)^4 3p\pi_u, \tag{1}$$

$$o\,^1\Pi_u, F\,^3\Pi_u: \cdots (2\sigma_u)^2(3\sigma_g)^2(1\pi_u)^3 3s\sigma_g, \tag{2}$$

$$b\,^1\Pi_u, C\,^3\Pi_u: \cdots (2\sigma_u)(3\sigma_g)^2(1\pi_u)^4(1\pi_g), \tag{3}$$

$$b\,^1\Pi_u, C\,^3\Pi_u, C'\,^3\Pi_u: \cdots (2\sigma_u)^2(3\sigma_g)(1\pi_u)^3(1\pi_g)^2, \tag{4}$$

where $\cdots$ represents the $(1\sigma_g)^2(1\sigma_u)^2(2\sigma_g)^2$ occupancies common to all of the MOs. The *c* and *G* states are members of the $np\pi_u$ Rydberg series, converging on the $X\,^2\Sigma_g^+$ ground state of the molecular ion, while the *o* and *F* states are members of the $ns\sigma_g$ Rydberg series, converging on the $A\,^2\Pi_u$ first-excited state. The MO configuration (4) gives rise to three $^1\Pi_u$ states and four $^3\Pi_u$ states.[17] The *b* and *C* states both have unusually shaped potential-energy curves (see Fig. 1), displaying a marked change from the valence-hole configuration (3) to the valence configuration (4), as *R* increases through 1.3–1.4 Å.[2] In the region $R\approx 1.5$ Å, the C' and *C* states can be thought of as the lowest two $^3\Pi_u$ states associated with MO configuration (4), while the *b* state is the lowest $^1\Pi_u$ state associated with configuration (4), since the C' state has no singlet analogue. All pairs of the MO configurations (1)–(4) differ in exactly two of the occupied electron orbitals, leading to the possibility of strong electrostatic interactions between the associated electronic states of like symmetry,[7] including Rydberg-valence, Rydberg-Rydberg, and valence-valence interactions. Indeed, the interactions between configurations (3) and (4) are already apparent in the shapes of the *b*- and *C*-state potentials in Fig. 1. The remaining interactions between our chosen diabatic-basis states are considered explicitly in what follows.

1. The $^1\Pi_u$ states

The strong Rydberg-valence and Rydberg-Rydberg interactions between the N_2 states of $^1\Pi_u$ symmetry were first treated semiempirically in the seminal paper by Stahel *et al.*,[18] who produced a comprehensive diabatic model of the coupled states which was able to reproduce the experimental level energies and rotational constants to within $\sim 10\ cm^{-1}$ rms and $\sim 0.05\ cm^{-1}$ rms, respectively, and also explain the many intensity anomalies observed in the $b \leftarrow X$, $c \leftarrow X$, and $o \leftarrow X$ systems. Recently, this model has been superseded by the *ab initio* semiempirical study of Spelsberg and Meyer,[19] who employed *R*-dependent couplings and obtained improved agreement with experiment, with rms discrepancies in energies and rotational constants of only $\sim 2\ cm^{-1}$ rms and $\sim 0.006\ cm^{-1}$ rms, respectively, in the energy range $100\,810-114\,300\ cm^{-1}$. The model of Spelsberg and Meyer[19] differs from that of Stahel *et al.*[18] in some significant aspects. First, the Rydberg-valence coupling H_{bo}^{el} is much greater in Ref. 18 than in Ref. 19, while the reverse is true for the Rydberg-Rydberg coupling H_{co}^{el}. Second, the Rydberg electronic transition moment M_{oX} is much smaller in Ref. 18 than in Ref. 19. Finally, the sense of the interference effect between the $o \leftarrow X$ and $b \leftarrow X$ diabatic transition amplitudes is *constructive*, according to Stahel *et al.*,[18] but *destructive*, according to Spelsberg and Meyer.[19] The extent to which these differences are a result of the use of *R*-dependent couplings and electronic transition moments by Spelsberg and Meyer[19] is unclear. Here, we build on the significant progress made in these two previous works, adopting the diabatic $^1\Pi_u$ model of Spelsberg and Meyer[19] as the starting point for our consideration of the *b*, *c*, and *o* states and their mutual interactions.

Initially, we constructed a three-channel CSE model for these $^1\Pi_u$ states and compared computed energies and rotational constants with an experimental database, compiled by critically assessing available data for $^{14}N_2$,[3,8,9,14,20–27] $^{15}N_2$,[28] and $^{14}N^{15}N$,[28] in the $100\,800-116\,400\ cm^{-1}$ energy range, sometimes with the aid of new rotational analyses. In order to minimize the influence of rotational interactions with $^1\Sigma_u$ states, which were excluded from our model, the rotational constants in the experimental database were those pertaining to the *f*-parity levels, which are unaffected by interactions with the $^1\Sigma_u^+$ states in this energy region.[29] For the most part, our adopted experimental values are similar to those employed both by Stahel *et al.*[18] and Spelsberg and Meyer,[19] except in the case of the mutually interacting $o(v=1)$ and $b(v=9)$ levels of $^{14}N_2$, where both previous works incorrectly used the *deperturbed* constants, rather than the actual (perturbed) constants,[30] despite the fact that their models inherently include the effects of this interaction. This led to significant discrepancies between their model results for these levels and experiment, especially in the case of the rotational constants.

By adjusting the *b*, *c*, and *o* potential-energy curves[31] and scaling the *R*-dependent couplings of Spelsberg and Meyer,[19] we obtained significantly improved performance of the model in reproducing the experimental database. This resultant three-channel CSE model of the $^1\Pi_u$-state spectroscopy was then employed in the initial stages of the construction of the full predissociation model discussed in Sec. II B.

2. The $^3\Pi_u$ states

In the energy range below the $^4S+^2D$ dissociation limit at $97\,938 \pm 40\ cm^{-1}$,[32] the spectroscopy of the *C* and *C'* triplet states has been well characterized. The best insight into the structure of these states and their strong mutual interaction, which is responsible for a rapidly increasing perturbation in the energies, *B* values, and *D* values for the *C*-state levels as *v* increases from 0 to 4, was first provided in a key paper by Carroll and Mulliken,[17] who also arranged observations from a number of sources into a picture of the more highly coupled *C* and *C'* levels at slightly higher energies. Ledbetter and Dressler[33] attempted to quantify the $C \sim C'$ interaction semiempirically, using a diabatic two-state analysis of the experimental information available at the time. They deduced an electronic interaction matrix element $H_{CC'}^{el} \approx 700\ cm^{-1}$, assumed to be *R* independent. However, their determination suffered from a lack of data on the $C(v=5)$ level, which was observed soon after by Ledbetter.[34] Robbe[6] performed an early *ab initio* calculation of the $^3\Pi_u$ states of N_2, obtaining a value of $H_{CC'}^{el} \approx 1000\ cm^{-1}$. More recently, adiabatic potential-energy curves for the $^3\Pi_u$ states, resulting from the *ab initio* calculations of Guberman,[35] and Partridge,[4] have indicated a strong inflection on the outer limb of the *C*-state potential due to the configurational change discussed above (see Fig. 1). This characteristic, not so evident in the work of Robbe,[6] will prove to be crucial here in explaining the observed predissociation pattern for the $^1\Pi_u$ levels of N_2.

The *F* and *G* Rydberg states have not been at all well characterized experimentally, but are expected to participate in strong Rydberg-valence interactions with the *C* and *C'* states, analogous to those observed for the $^1\Pi_u$ states. In order to minimize model complexity, and avoid the uncertainty regarding the roles of these states in the N_2 predissociation, we have excluded the *F* and *G* states from our CSE model, restricting ourselves to a study of the lowest vibrational levels of the $^1\Pi_u$ manifold, below $\sim 105\,500\ cm^{-1}$. Although this region contains the $v=0$ levels of both the *F* and *G* states,[10] an inspection of Fig. 1 indicates that these levels are unlikely to be heavily predissociated by the *C'* continuum, lying well below the relevant potential-energy-curve crossing points. Thus, in a simple picture, these low levels should not strongly disrupt the structure of the $^3\Pi_u$ continuum and provide dominant pathways for the $^1\Pi_u$ predissociation, although the likely strong $F \sim G$ Rydberg-Rydberg interaction and associated level mixing may modify this conclusion somewhat.

Initially, we constructed a two-channel diabatic CSE model of the interacting states $C\ ^3\Pi_{u1}$ and $C'\ ^3\Pi_{u1}$ and iteratively compared computed energies and rotational constants for the *f*-parity levels with an experimental database compiled from the works of Tilford *et al.*[36] $[C(v=0-4)]$, Ledbetter[34] $[C(v=5)]$, Carroll[37] $[C'(v=0)]$, Ledbetter and Dressler[33] $[C'(v=1)]$, and Tanaka and Jursa[38] $[C'(v=2)]$. Our initial diabatic potential-energy curves were deduced

from the adiabatic curves of Partridge.[4] By adjusting the C and C' potentials and their mutual electrostatic coupling, assumed to be R independent, it was a simple matter to obtain good agreement with the experimental database. This resultant two-channel model of the $^3\Pi_u$ spectroscopy was then employed in the initial stages of the construction of the full predissociation model discussed in Sec. II B.

B. Spin-orbit interactions and predissociation

As mentioned in Sec. I, the $^1\Pi_u$ predissociation mechanism in N_2 cannot be of the allowed type, including electrostatic. In this study, we consider only band-head linewidths, thus approximating the rotationless situation. Therefore, the applicable predissociation mechanism must involve (homogeneous) spin-orbit interactions with triplet states ($\Delta\Lambda=0,\pm1,\Delta S=1,\Delta\Omega=0$).[7] None of the $^3\Sigma_u^\pm$ states of N_2 is energetically capable of predissociating the $^1\Pi_u$ manifold, with the exception of the second $^3\Sigma_u^+$ state,[39] whose repulsive potential-energy curve crosses that of the b state high enough on its outer limb so as to not affect the low vibrational levels which are the subject of this work. Thus, it is necessary here only to consider spin-orbit interactions with $^3\Pi_u$ states.

In the case of the $b\ ^1\Pi_u$ state, we must consider interactions with both the $C\ ^3\Pi_u$ and $C'\ ^3\Pi_u$ states, which lead to indirect and direct predissociation mechanisms, respectively. One would expect a significant spin-orbit interaction between the b and C valence states which are, effectively, isoconfigurational. For $R\lesssim1.35$ Å, both states are derived mainly from the $\sigma_u\pi_g$ MO configuration (3), leading to the crude estimate:[7,36]

$$H_{bC}^{\mathrm{so}}=\langle b\ ^1\Pi_{u1}|\mathbf{H}^{\mathrm{so}}|C\ ^3\Pi_{u1}\rangle\approx A(C\ ^3\Pi_u)\approx\ +39\ \mathrm{cm}^{-1}. \tag{5}$$

It is not possible simply to estimate $H_{bC'}^{\mathrm{so}}$ in a similar fashion because of the strong mixing between the states derived from MO configuration (4). However, Robbe[6] obtained the values $H_{bC}^{\mathrm{so}}=25\ \mathrm{cm}^{-1}$ and $H_{bC'}^{\mathrm{so}}=10\ \mathrm{cm}^{-1}$ in his early *ab initio* study.[40]

In the case of the Rydberg states of $^1\Pi_u$ symmetry, isoconfigurational spin-orbit interactions with their $^3\Pi_u$ counterparts must be considered. The diabatic $c\ ^1\Pi_u$ and $G\ ^1\Pi_u$ states arise from the $\sigma_g3p\pi_u$ MO configuration (1), leading to the estimate:[7,41]

$$H_{cG}^{\mathrm{so}}=\langle c\ ^1\Pi_{u1}|\mathbf{H}^{\mathrm{so}}|G\ ^3\Pi_{u1}\rangle\approx A(G\ ^3\Pi_u)=a_{3p\pi_u}\approx\zeta_{3p_N}\approx\ +2\ \mathrm{cm}^{-1}. \tag{6}$$

The diabatic $o\ ^1\Pi_u$ and $F\ ^3\Pi_u$ states arise from the $\pi_u^3 3s\sigma_g$ MO configuration (2), leading to the estimate:[7,42]

$$H_{\mathrm{of}}^{\mathrm{so}}=\langle o\ ^1\Pi_{u1}|\mathbf{H}^{\mathrm{so}}|F\ ^3\Pi_{u1}\rangle\approx A(F\ ^3\Pi_u)\approx\tfrac{1}{2}A[N_2^+(A\ ^2\Pi_u)]\approx-37\ \mathrm{cm}^{-1}. \tag{7}$$

From Eq. (6), the $c\sim G$ interaction is very weak and unlikely to contribute to the c-state predissociation, especially taking into account the extremely indirect nature of such a predissociation mechanism, so the omission of the G state from our CSE model should not directly affect the c-state level widths. On the other hand, from Eq. (7), the $o\sim F$ interaction is fairly strong and likely to affect, in particular, the o-state predissociation. Therefore, since we also omit the F state from our CSE model, we do not consider o-state level widths as part of this study, which is restricted to levels below $o(v=0)$ at $\sim105\,700\ \mathrm{cm}^{-1}$, i.e., $b(v=0-6)$ and $c(v=0)$.

Finally, we combined the three-channel $^1\Pi_{u1}$ and two-channel $^3\Pi_{u1}$ CSE models described in Secs. II A 1 and II A 2, respectively, into a five-channel model of the Π_{u1} spectroscopy and predissociation, by including the H_{bC}^{so} and $H_{bC'}^{\mathrm{so}}$ spin-orbit interactions, assumed to be R independent. Since we were not concerned with intensities, the diabatic electronic transition moments of Spelsberg and Meyer[19] were adopted without further optimization. In this picture, the only nonzero diabatic electronic transition moments are for the b-X, c-X, and o-X allowed transitions, transitions into the $^3\Pi_{u1}$ states borrowing intensity from the allowed transitions through $^3\Pi_{u1}\sim{}^1\Pi_{u1}$ spin-orbit mixing.

The b, c, o, C, and C' potential-energy curves, in their appropriate regions of sensitivity, together with the electrostatic interactions H_{bc}^{el}, H_{co}^{el}, H_{bo}^{el}, and $H_{CC'}^{\mathrm{el}}$, and the spin-orbit interactions H_{bC}^{so} and $H_{bC'}^{\mathrm{so}}$, were adjustable parameters determined in a least-squares fitting procedure where the model energies, rotational constants,[43] and predissociation linewidths, obtained from profile analyses of the resonances in the computed CSE photodissociation cross section, were compared with an experimental database. The spectroscopic database has been described in Secs. II A 1 and II A 2. In the case of the $^1\Pi_u$ predissociation linewidths, we relied principally on the high-resolution, laser-based, isotopic band-head results discussed in the companion paper, Ref. 11 [$^{14}N_2, b(v=0,5,6), c(v=0)$; $^{15}N_2, b(v=0-4,6), c(v=0)$; $^{14}N^{15}N, b(v=0,1,5,6), c(v=0)$], together with a value for $^{14}N_2, b(v=4)$ from Ref. 20. For the $b(v=2,3)$ levels of $^{14}N_2$, we used new band-head linewidths determined by profile-fitting the synchrotron-based photoabsorption spectra of Stark.[14] Finally, for the narrow levels $^{14}N_2, b(v=1)$ and $^{15}N_2, b(v=5)$, we used linewidths deduced from the laser-based pump-probe lifetimes of Refs. 12 and 13, respectively. It should be noted that our adopted values are the considered result of a critical analysis of data from many sources, data which often contain significant disagreements, largely because of the difficulty of measuring linewidths which span many orders of magnitude, combined with an overoptimistic assessment of experimental resolution in some cases.

III. RESULTS AND DISCUSSION

A. Model parameters

The diabatic $^1\Pi_u$ and $^3\Pi_u$ potential-energy curves determined as a result of the least-squares fitting procedure are shown in Fig. 2. The $^1\Pi_u$ potentials (solid curves) differ only marginally from the semiempirical potentials of Spelsberg and Meyer,[19] those differences occurring principally because of the different methods employed in the computation of the

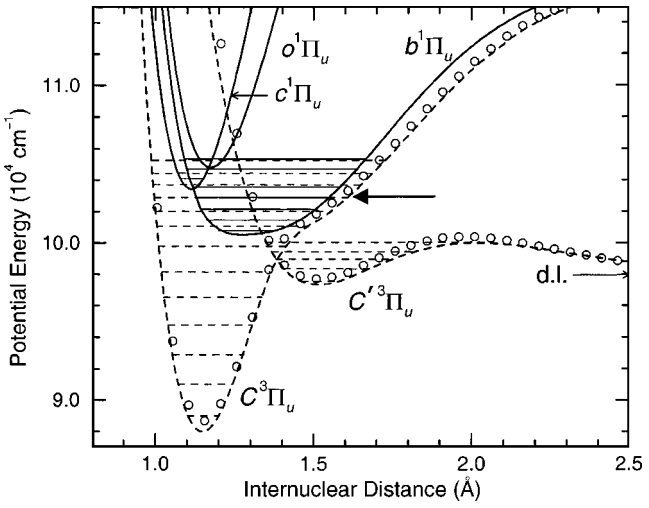

FIG. 2. Diabatic potential-energy curves used in the CSE predissociation model, referred to the $v=0$, $J=0$ level of the $X\,^1\Sigma_g^+$ ground state (not shown). Solid curves: $^1\Pi_u$ states. Dashed curves: $^3\Pi_u$ states. Vibrational levels for the coupled states are also indicated, located in the potential wells appropriate to their dominant character. Solid lines: $^1\Pi_u$ levels. Dashed lines: $^3\Pi_u$ levels. The crucial degeneracy between $b(v=3)$ and $C(v=9)$ is highlighted by a solid arrow. A comparison is also made with $^3\Pi_u$ potentials deduced from the *ab initio* calculations of Partridge (open circles, Ref. 4).

coupled-channel energies. In addition, we have not been restricted by the use of analytic descriptions of the potentials (see Sec. II A 1).

Part of the significant progress made in this work is the determination of the $^3\Pi_u$ potentials (dashed curves in Fig. 2). In the region below $\sim 98\,500$ cm^{-1}, this determination is straightforward. However, due to the current lack of experimental information on the C-state levels above this energy [but see later comments on $C(v=7,8)$], the outer limb of the C-state potential-energy curve in the $R=1.4-1.7$ Å region has been determined essentially *indirectly*, largely through its effect on the b-state linewidths. The resulting curve in this region is relatively smooth, and exhibits an inflection similar to that in the *ab initio* curve of Partridge.[4] This behavior is extremely gratifying and lends credence both to our adopted linewidth database, and to our resultant predissociation model, which, as we shall see, predicts an indirect predissociation mechanism based on the $b\sim C$ interaction. If the outer limb of the C-state potential were taken to have no inflection and cross the b state, as in several earlier works,[5,6,33] then there is *no possibility* that the relative vibrational-level spacings of the b and C states would allow the experimental b-state widths to be reproduced by such a CSE model. Finally, we note that the model diabatic $^3\Pi_u$ potential-energy curves differ systematically from those implied by the multireference configuration-interaction (plus Davidson correction) (MRCI+Q) *ab initio* calculations of Partridge (dashed curves in Fig. 2),[4] displaying slightly greater well depths and lying to slightly smaller internuclear distances, while displaying good overall agreement. These differences are typical of those usually observed between MRCI+Q and experimentally based potentials. For example, a shift to smaller R by 3.3 mÅ, together with an increase in well depth by 2.4%, produces excellent agreement between the *ab initio* and model C-state potentials in the region of their minima. These adjustments are remarkably similar to those required in the case of the Herzberg states of O_2.[44]

The model diabatic electrostatic couplings H_{bc}^{el}, H_{bo}^{el}, and H_{co}^{el}, determined in the fitting procedure by scaling the R-dependent couplings of Spelsberg and Meyer,[19] and principally sensitive to the $^1\Pi_u$ spectroscopic fitting (see Sec. II A 1), are 102%, 85%, and 97%, respectively, of the recommended values of Ref. 19. The model diabatic electrostatic coupling $H_{CC'}^{\mathrm{el}}$, principally sensitive to the $^3\Pi_u$ spectroscopic fitting (see Sec. II A 2), is 810 ± 20 cm^{-1},[45] significantly exceeding the previous semiempirical estimate of ~ 700 cm^{-1},[33] which was based on a less complete experimental database. Our value of $H_{CC'}^{\mathrm{el}}$ is of the same order of magnitude as Robbe's *ab initio* calculation of the electrostatic interaction between the lowest $^3\Pi_u$ states derived from the MO configurations (3) and (4), respectively, which yielded an estimate of ~ 1000 cm^{-1},[6] and is fairly consistent with half of the minimum separation between the adiabatic C and C' potential-energy curves of Partridge.[4,46]

The model diabatic spin-orbit couplings H_{bC}^{so} and $H_{bC'}^{\mathrm{so}}$, principally sensitive to the $^1\Pi_u$ linewidth fitting, are 46 ± 2 cm^{-1} and -1.3 ± 0.5 cm^{-1}, respectively. Our value of H_{bC}^{so} significantly exceeds Robbe's *ab initio* value of 25 cm^{-1},[6] but, somewhat surprisingly, is in quite good agreement with the single-configuration estimate of 39 cm^{-1} [Eq. (5)]. Our value of $H_{bC'}^{\mathrm{so}}$ is not very well determined, but its magnitude is, nevertheless, significantly smaller than the 10 cm^{-1} *ab initio* value of Robbe.[6]

Recently, one of us (J-M.R.) has updated these *ab initio* calculations, obtaining MRCI potential-energy curves for the C and C' states in the region of their avoided crossing, and an R-dependent spin-orbit interaction matrix element between the b state and the lowest adiabatic state of $^3\Pi_u$ symmetry. These results are much more consistent with our model determinations. First, the minimum separation between the MRCI C- and C'-state potentials implies that $H_{CC'}^{\mathrm{el}}\approx 770$ cm^{-1}. Second, the adiabatic spin-orbit interaction matrix element is consistent with a diabatic $H_{bC}^{\mathrm{so}}\approx 43$ cm^{-1}, with little R dependence, together with a diabatic $H_{bC'}^{\mathrm{so}}$ which increases strongly in magnitude as R increases, but which has an absolute value near -1 cm^{-1} at $R=1.34$ Å, the crossing point between the b and C' states. Since it is the value at this crossing point which will influence the direct predissociation mechanism of the b state by the C' state, and thus be returned by our CSE-model fitting procedure, there is thus remarkably good agreement between all the model interactions and the *ab initio* calculations. Both determinations imply that the matrix-element product $H_{bC}^{\mathrm{so}}H_{CC'}^{\mathrm{el}}H_{bC'}^{\mathrm{so}}$ is *negative*.

B. Energies and linewidths

1. The $^1\Pi_u$ states

Spectroscopic constants and predissociation widths for the lowest $^1\Pi_u$ levels, computed using the five-channel CSE model, are compared with the experimental database in Table I. The coupled-channel energies for the $^1\Pi_u$ levels are also illustrated in Fig. 2 as solid lines, associated with the diabatic potential-energy curve providing the dominant character of

TABLE I. Comparison of experimental and coupled-channel spectroscopic constants and predissociation linewidths for the lowest $^1\Pi_u$ levels of isotopic N_2.

Isotope	Level	T_{expt}[a]	T_{CSE}[a]	ΔT	B_{expt}[b]	B_{CSE}[b]	ΔB	Γ_{expt}[c]	Γ_{CSE}[c]	Γ^C_{CSE}
$^{14}N_2$	$b(0)$	100 816.8[d]	100 816.4	−0.4	1.447[d]	1.447	0.000	0.17(2)[e]	0.16	0.19
	$b(1)$	101 451.6[f]	101 451.4	−0.2	1.408[f]	1.409	0.001	0.0006(3)[g]	0.0000	0.0004
	$b(2)$	102 151.7[h]	102 151.7	0.0	1.387[h]	1.391	0.004	0.64(6)[i]	0.61	0.67
	$b(3)$	102 861.3[j]	102 861.6	0.3	1.394[j]	1.387[k]	−0.007[k]	3.3(2)[j]	3.3	3.4
	$b(4)$	103 548.8[l]	103 548.8	0.0	1.423[l]	1.426	0.003	0.29(2)[f]	0.26	0.28
	$c(0)$	104 138.5[m]	104 138.5	0.0	1.507[m]	1.503	−0.004	0.079(7)[e]	0.082	0.093
	$b(5)$	104 699.7[n]	104 700.0	0.3	1.429[n]	1.427	−0.002	0.022(5)[e]	0.018	0.015
	$b(6)$	105 346.0[o]	105 346.2	0.2	1.362[o]	1.363	0.001	0.015(4)[e]	0.015	0.020
$^{15}N_2$	$b(0)$	100 843.4[p]	100 843.8	0.4	1.346[p]	1.351	0.005	0.13(3)[e]	0.14	0.13
	$b(1)$	101 455.8[p]	101 456.1	0.3	1.315[p]	1.317	0.002	0.16(3)[e]	0.16	0.17
	$b(2)$	102 128.9[p]	102 129.0	0.1	1.298[p]	1.302	0.004	0.77(9)[e]	0.83	0.90
	$b(3)$	102 817.9[p]	102 817.7	−0.2	1.292[p]	1.296	0.004	0.69(9)[e]	0.69	0.70
	$b(4)$	103 485.4[p]	103 485.4	0.0	1.320[p]	1.324	0.004	0.53(11)[e]	0.40	0.39
	$c(0)$	104 069.9[p]	104 070.2	0.3	1.397[p]	1.395	−0.002	0.18(3)[e]	0.18	0.20
	$b(5)$	104 613.2[p]	104 613.5	0.3	1.344[p]	1.345	0.001	0.0051(25)[q]	0.0034	0.0024
	$b(6)$	105 234.7[p]	105 234.9	0.2	1.269[p]	1.269	0.000	0.0054(25)[e]	0.0031	0.0055
$^{14}N^{15}N$	$b(0)$	100 830.2[d]	100 830.3	0.1	1.401[d]	1.400	−0.001	0.065(21)[e]	0.060	0.076
	$b(1)$	101 453.7[d]	101 453.7	0.0	1.362[d]	1.363	0.001	0.028(16)[e]	0.039	0.045
	$c(0)$	104 104.9[p]	104 105.0	0.1	1.455[p]	1.449	−0.006	0.11(3)[e]	0.11	0.12
	$b(5)$	104 656.9[p]	104 657.1	0.2	1.389[p]	1.386	−0.003	≲0.006[e]	0.0079	0.0063
	$b(6)$	105 291.2[p]	105 291.5	0.3	1.315[p]	1.315	0.000	0.0074(29)[e]	0.0063	0.0095
				0.2 rms			0.003 rms			

[a] T_{v0}, in cm^{-1}.
[b] Effective f-level rotational constant for $J \leq 5$, in cm^{-1}.
[c] Low-J predissociation linewidth, in cm^{-1} FWHM. Experimental linewidths have been corrected for the radiative contribution, assumed to be 0.0014 cm^{-1} (Ref. 12). Values in parentheses are the 1σ experimental uncertainties, in units of the last significant figure. The Γ_{CSE} are full-model widths, while the Γ^C_{CSE} were computed without any direct predissociation by the C' state.
[d] Reference 8.
[e] Reference 11.
[f] Reference 20.
[g] Reference 12.
[h] Reference 3.
[i] Reference 14.
[j] Deduced from spectra of Ref. 14.
[k] If triplet structure is included for the C and C' states (see discussion in text), the computed B value for $b(3)$ becomes 1.395 cm^{-1}, in much better agreement with experiment. ΔB for this level has been omitted in the determination of the rms discrepancy.
[l] Deduced from spectra of Ref. 21.
[m] Reference 22.
[n] Deduced from term values of Ref. 24.
[o] Reference 25.
[p] Reference 28.
[q] Reference 13.

the level. In the case of the spectroscopic-constant database, the principal difference between our values for $^{14}N_2$ and those adopted by Stahel *et al.*,[18] and Spelsberg and Meyer,[19] occurs for $b(v=3)$, where we have determined actual constants from a photoabsorption spectrum due to Stark,[14] rather than using the deperturbed constants of Carroll and Collins.[3] As noted by Carroll and Collins,[3] $b(v=3)$ is perturbed by a higher-lying level, which we will show below to be $C(v=9)$. Since we include the $^1\Pi_{u1} \sim {}^3\Pi_{u1}$ interactions in our model, we must compare with perturbed experimental data, rather than the deperturbed data necessary for models of the $^1\Pi_u$ states alone.

This study represents the first optimization of the $^1\Pi_u$ states of N_2 which includes these singlet-triplet interactions, and the first to simultaneously fit data for all isotopomers. The agreement between the experimental and CSE-model spectroscpic constants in Table I is excellent, with root-mean-square discrepancies of only 0.2 cm^{-1} in the energies, and 0.003 cm^{-1} in the B values. This performance is superior to the $^{14}N_2$-based model of Ref. 19, mainly due to increased flexibility in the shape of the b-state potential-energy curve. Parts of the small differences between the CSE-model $^1\Pi_u$ potentials and those of Ref. 19 arise from the H^{so}_{bC} interaction, which causes small shifts in the b-state level energies, in the range 0–3 cm^{-1}.

As has been demonstrated in the companion paper, Ref. 11, the $^1\Pi_u$ experimental linewidths display complex patterns of dependence on vibrational quantum number and isotopic mass, patterns which prove to be challenging to reproduce. In Table I, the experimental predissociation linewidth database is based on experimental bandhead (low J) widths, corrected for the radiative contribution.[47] This correction is of importance principally for the radiatively dominated $b(v=1)$ level of $^{14}N_2$, which has been discussed in detail in Ref.

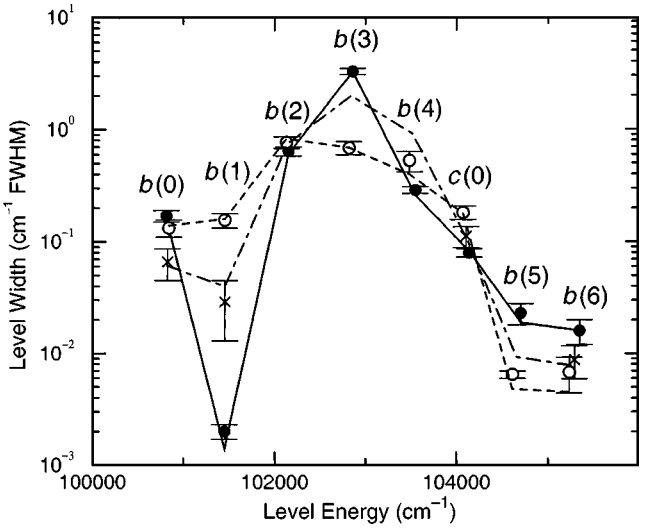

FIG. 3. Comparison between model CSE (line vertices) and experimental (symbols) widths for the lowest $^1\Pi_u$ levels of isotopic N_2. Solid line, filled circles: $^{14}N_2$. Dot-dashed line, crosses: $^{14}N^{15}N$. Dashed line, open circles: $^{15}N_2$. For ease of presentation, a radiative contribution, assumed to be 0.0014 cm^{-1} FWHM (Ref. 12), has been added to the computed predissociation widths of Table I.

12. The CSE-model rotationless widths (penultimate column in Table I) are in very good agreement with the experimental values. This degree of agreement is extremely gratifying, considering the vibrational and isotopic complexity, together with the many orders of magnitude spanned by the widths, lending significant credibility to the CSE model. Comparisons between the computed and experimental vibrational and isotopic dependences are shown more clearly in Fig. 3, where, for clarity of presentation, the total widths are shown, the computed predissociation widths having been corrected upwards by the radiative contribution. For example, the interesting isotopic behavior of the $b(v=0)$ linewidth in Fig. 3, which goes through a minimum for $^{14}N^{15}N$, as the mass increases from $^{14}N_2$ to $^{15}N_2$, together with the dramatically increasing linewidth for $b(v=1)$ under the same circumstances, are evidently well reproduced by the CSE model. The linewidths predicted by the model for $^{14}N^{15}N$, $b(v=2,3,4)$ are 0.75, 2.0, and 0.92 cm^{-1} FWHM, respectively. These large widths, together with the low abundance of this isotopomer, explain why Sprengers *et al.*[11] were unable to detect these levels with adequate signal-to-noise ratio in their 1+1-photon ionization spectra.

While the emphasis here is on the rotationless linewidths, mainly because of the uncertain role of rotational coupling to $^1\Sigma_u^+$ states in the $^1\Pi_u$ predissociation, together with the exclusion of these states from our CSE model, it is nevertheless of interest qualitatively to consider the dependence of the predissociation linewidths on J for the lowest vibrational levels, which are those least likely to be affected significantly by such interactions. Stark[14] has found experimentally that, while the $b(v=4)$ width for $^{14}N_2$ shows little J dependence, both the $b(v=2$ and $3)$ widths appear to *decrease* significantly with J. A qualitative decrease in the case of $b(v=3)$ had also been suggested previously.[3] Five-channel CSE-model calculations performed for nonzero J values are in broad agreement with the observations of Stark,[14] for $b(v=2$ and $4)$, but disagree completely in the case of $b(v=3)$, where the model predicts a strong *increase* in width as J increases. In view of the success of the model in explaining all other observations, this disagreement is potentially serious and merits investigation. Its explanation lies in the combination of the neglect of the triplet structure of the C state in the model and the small separation in energy between $b(v=3)$ and its perturber $C(v=9)$. We performed a test calculation, including all Ω components of the C and C' states, together with their corresponding **S**-uncoupling interactions, in a nine-channel CSE model, and all difficulties disappeared: the computed $b(v=3)$ level width now *decreased* strongly at intermediate and high J values, in qualitative agreement with the experimental observations. Furthermore, the computed B value for $b(v=3)$ increased from 1.387 cm^{-1} to 1.395 cm^{-1}, in much better agreement with the experimental value of 1.394 cm^{-1} (see Table I).

This result for the J dependence of the linewidth may be qualitatively understood as follows. If the triplet structure of the C state is ignored, then, taking into account the relative energies and rotational constants of the levels (see Tables I and II), as J increases, the heavily predissociated $C(v=9)$ approaches $b(v=3)$ from above, the resultant increasing coupling likely to result in increasing "borrowing" of the $C(v=9)$ width by $b(v=3)$, consistent with the five-channel CSE-model result. In reality, however, even at quite low J the $b(v=3)$ level lies *within* the $C(v=9)$ triplet level structure. Thus, the $b(v=3)$ level width borrowed from $C(v=9)$ is sensitively dependent on the degree of mutual coupling between the three $^3\Pi_u$ sublevels, which increases with J, together with the individual energy differences between the singlet level and the triplet sublevels, which also change rapidly with J. These sensitivities, to an extent, can give rise to destructive quantum-interference effects in the calculated widths. Thus, the C-state triplet structure *must* be considered in the case of $b(v=3)$, necessitating the use of the full nine-channel CSE model, which happens to reproduce the correct J dependence. Normally, e.g., as in the predissociation of $b(v=2)$, all components of the nearest triplet perturbing level are well separated from the perturbed singlet level and the five-channel CSE model provides an adequate description of the J dependence of the predissociation.

2. The $^3\Pi_u$ states

In Table II, a comparison is made between the experimental database for the $^3\Pi_u$ levels of $^{14}N_2$ and five-channel CSE-model computations. The coupled-channel energies for the $^3\Pi_u$ levels are also illustrated in Fig. 2 as dashed lines, associated with the diabatic potential-energy curve providing the dominant character of the level. We consider the $^3\Pi_u$ levels in three groups.

First, in the case of the well-known bound levels $C(v=0-5)$ and $C'(v=0-2)$, below $\sim$98 950 cm^{-1}, excellent agreement is found between the experimental energies and B values and the corresponding model values. The strong mixing of the C and C' levels above $C'(v=0)$ leads to perturbations in T and B which are well reproduced by the model, leading, in fact, to the reasonably precise value for $H_{CC'}^{el}$,

TABLE II. Experimental and coupled-channel spectroscopic constants and predissociation linewidths for the lowest $^3\Pi_{u1}$ levels of $^{14}N_2$.

Level	T_{expt}[a]	T_{CSE}[a]	ΔT	B_{expt}[b]	B_{CSE}[b]	ΔB	Γ_{expt}[c]	Γ_{CSE}[c]
$C(0)$	88 977.9[d]	88 977.9	0.0	1.815[d]	1.815	0.000		0.000
$C(1)$	90 972.3[d]	90 972.3	0.0	1.793[d]	1.793	0.000		0.000
$C(2)$	92 913.1[d]	92 913.2	0.1	1.769[d]	1.769	0.000		0.000
$C(3)$	94 787.1[d]	94 787.0	−0.1	1.740[d]	1.741	0.001		0.000
$C(4)$	96 568.4[d]	96 568.5	0.1	1.700[d]	1.700	0.000		0.000
$C'(0)$	97 562.3[e]	97 562.3	0.0	1.049[e]	1.050	0.001		0.000
$C(5)$	98 131[f]	98 131	0	1.409[f]	1.409	0.000		0.000
$C'(1)$	98 358.1[g]	98 357.9	−0.2	1.218[g]	1.218	0.000		0.000
$C'(2)$	98 942[h]	98 942	0		1.019			0.000
$C'(3)$[i]		99 448			1.04			0.006
$C(6)$[i]		99 793			1.11			3
$C'(4)$[i]		100 045[j]			0.98[j]			89[j]
$C(7)$	101 066[k]	101 065	−1.0		1.39		∼10–35[k]	13
$C(8)$	102 051[k]	102 047	−4.0		1.30		∼10–50[k]	16
$C(9)$		102 888[j]			1.33[j]			86[j]
$C(10)$[l]		103 693[j]			1.34[j]			152[j]
$C(11)$[l]		104 471[j]			1.30[j]			149[j]
$C(12)$[l]		105 239[j]			1.23[j]			105[j]

[a] T_{v0}, in cm^{-1}.
[b] Effective f-level rotational constant for $J \leqslant 5$, in cm^{-1}.
[c] Low-J predissociation linewidth, in cm^{-1} FWHM.
[d] Reference 36.
[e] Reference 37.
[f] Reference 34.
[g] Reference 33.
[h] Deduced from band heads of Ref. 38.
[i] Constants and widths increasingly approximate for these levels which are dependent on the shape of the outer limb and hump on the C' potential-energy curve. The uncertainty in the energy of $C'(4)$, e.g., could be on the order of 100 cm^{-1}.
[j] Computed value obtained by having a nonzero transition moment only to the C state in the coupled-channel model.
[k] Reference 14; approximate value deduced from broad feature in liquid-nitrogen-temperature spectrum of Ref. 23. The $C(7)$ level was also observed for $^{15}N_2$ at 100 898 cm^{-1}, with a width in the range ∼10–40 cm^{-1}. The corresponding computed energy is 100 903 cm^{-1}, with a FWHM width of 16 cm^{-1}.
[l] Constants and widths for these levels determined *indirectly* from fits to b-state linewidths. Actual values may be affected by interactions with the Rydberg F and G states, which are not included in the model.

reported in Sec. III A. Although $C(v=5)$ and $C'(v=1,2)$ lie above the $N(^4S)+N(^2D)$ dissociation limit, the computed predissociation widths for these rotationless levels are not significant.

Second, the CSE model predicts the existence of the predissociating levels $C(v=6)$ and $C'(v=3,4)$, in the energy region immediately below the hump in the C' potential near $R=2.0$ Å. These levels are not known experimentally, but are strongly mixed, as illustrated by the computed B values in Table II and the irregular level pattern in Fig. 2. These rotationless levels predissociate by tunneling through the C' hump, with a rapidly increasing probability as the energy increases, as confirmed by the computed predissociation widths in Table II. The predicted spectroscopic constants and widths for these particular levels are not very precise, the uncertainty increasing significantly with energy, since they are dependent on the details of the C' potential-energy curve in the region of $R=2.0$ Å, which is not well constrained by the fitting procedure. In the case of $C'(v=4)$, e.g., the uncertainty in energy may be on the order of 100 cm^{-1} or more, and, indeed, the existence of this particular level cannot be regarded as established at present. Nevertheless, the predictions of the current CSE model are consistent with the only experimental observations that are sensitive to this region of the C'-state potential, i.e., those of Hori and Endo,[48] who, in high-pressure emission spectra of the $C\,^3\Pi_u$-$B\,^3\Pi_g$ (second positive) system of N_2, noticed a complete breaking-off in the rotational structure, with last observed levels at $C(v=2,J=80)$ and $C(v=3,J=67)$. Carroll and Mulliken[17] interpreted this in terms of an electrostatic predissociation of the C state by the C' state, and another breaking-off occurring at lower J values,[49] which is suppressed at high pressures, in terms of weaker spin-orbit predissociation by a $^5\Pi_u$ state, also correlating with the $N(^4S)+N(^2D)$ dissociation limit. Our CSE model yields approximate FWHM predissociation widths for $C(v=2;J=79,80,81)$ of 0.002, 0.007, and 0.06 cm^{-1}, respectively, and for $C(v=3;J=66,67,68)$ of 0.0005, 0.02, and 1 cm^{-1}, respectively, first exceeding the radiative width of ∼0.0014 cm^{-1} FWHM (Ref. 32) at $v=2,J=79$, and $v=3,J=66$, thus in quite good agreement with experiment. Unfortunately, the widths associated with the weaker $^5\Pi_u$-induced predissociation are unknown, but our results would be in complete agreement with the experimental breaking-off points if those widths were on the order of 0.01 cm^{-1} FWHM, a not-unreasonable value.

Third, the levels $C(v=7-12)$ lie above both the $N(^4S)+N(^2D)$ dissociation limit and the C' potential hump, overlapping the energy range of the $^1\Pi_u$ levels studied here (see Fig. 2). The energies, rotational constants, and predissociation widths computed for these levels using the CSE model, shown in Table II, are, essentially, the indirect results of the

fitting process for the $^1\Pi_u$ linewidths. Prior to this work, none of these levels was known experimentally, but the preliminary predictions of our CSE model suggested that existing spectra should be reexamined for evidence of their existence. Stark[14] has reexamined some of the spectrographic plates of Yoshino,[23] taken for high column densities at liquid-nitrogen temperature, finding diffuse features corresponding to the $C\,^3\Pi_{u1}$-$X\,^1\Sigma^+_{g0}(7,0)$ and (8,0) subbands of $^{14}N_2$ and the (7,0) subband of $^{15}N_2$. Approximate experimental energies and width ranges for these features are listed in Table II, the maximum width defined by the approximate width of the low-temperature subband profile, the minimum width by the apparent lack of rotational stucture. The experimental energies for these levels were included in the final optimization of the CSE model, which yielded widths within the experimental ranges. The level $C(v=9)$ is a special case, almost coincident with $b(v=3)$. Due to this coincidence, it is unlikely that it will be possible to detect $C(v=9)$ in ground-state absorption spectra, but the CSE-model fits clearly place this level $\sim 26\ \mathrm{cm}^{-1}$ *above* $b(v=3)$. The spin-orbit mixing between these nearly degenerate levels, together with the strong predissociation of $C(v=9)$ by the C' continuum (computed predissociation width $86\ \mathrm{cm}^{-1}$ FWHM), are responsible for the large width of the $b(v=3)$ level in $^{14}N_2$. Model predictions for the $C(v=10-12)$ levels are included in Table II but we emphasise that these are indicative values only, since these levels may well be affected by interactions with the Rydberg F and G states, which are excluded from our model. Nevertheless, as we have shown in Sec. III B 1, the $^1\Pi_u$ width pattern is very well reproduced by this $^3\Pi_u$ energy and width pattern.

C. Predissociation mechanism

The large difference in magnitude between H^{so}_{bC} and $H^{\mathrm{so}}_{bC'}$, established in Sec. III A, suggests that the lowest $^1\Pi_u$ levels of N_2 are likely to be dominantly predissociated *indirectly* by the C' state, mediated by the H^{so}_{bC} spin-orbit and the $H^{\mathrm{el}}_{CC'}$ electrostatic interactions, rather than directly, due to the $H^{\mathrm{so}}_{bC'}$ spin-orbit interaction with the C' continuum. This conclusion has been confirmed unambiguously by the performance of CSE linewidth calculations in which the direct predissociation channel is artificially turned off, i.e., $H^{\mathrm{so}}_{bC'}=0$, the results of which, shown in the last column of Table I, differ little from the full-model results. Because of the dominance of the indirect channel, the expected quantum-interference effects between the direct and indirect predissociation channels are not too significant.

This study provides the first quantitative determination of the predissociation mechanism for the lowest $^1\Pi_u$ levels of N_2, a mechanism in agreement, somewhat ironically, with that proposed qualitatively as long ago as 1969 by Dressler,[2] and later espoused by Robbe.[6] The three relatively recent developments which have been pivotal to our success in establishing this mechanism have been (1) the photofragment-spectroscopic study of van der Kamp *et al.*,[10] which clearly shows that the $F\,^3\Pi_u$ state has no role to play in the predissociation of $b(v=3)$, contrary to the suggestion of Leoni and Dressler;[5] (2) sophisticated *ab initio* calculations of the $^3\Pi_u$ potential-energy curves[4,35] which reveal the inflection on the outer-limb of the C-state potential (see Sec. III A); and (3) an increased number of experimental linewidth measurements, of significantly improved dynamic range and precision, particularly those of Stark[14] and Sprengers *et al.*,[11] the latter of which are reported in the preceding paper in this issue, which enable much more rigorous testing of any proposed predissociation model.

Due the rather opaque nature of the CSE-model calculations, it is difficult to gain insight into the details of the N_2 predissociation process. However, an inspection of Fig. 2 reveals the essentials. There, it is seen that the interlacing of the b-state levels (solid lines) and the C-state levels (dashed lines) is such that a near degeneracy occurs between $b(v=3)$ and $C(v=9)$ in $^{14}N_2$, coinciding with the region of maximum predissociation. This result disagrees in detail with that of Robbe,[6] who, while proposing a similar predissociation mechanism, suggested that it was $C(v=8)$ which coincided with $b(v=3)$, largely due to the use of a C-state potential which lacked an outer-limb inflection, resulting in a C-state level pattern differing significantly from reality. Away from the $b(v=3)\sim C(v=9)$ degeneracy, the apparently chaotic accidental predissociation is a multilevel phenomenon, controlled by the separations and overlap factors between $^1\Pi_u$ and $^3\Pi_u$ level pairs, together with the C'-state-induced predissociation-width pattern of the C state (see final column of Table II).

The present study has been limited to levels below $o(v=0)$ at $\sim 105\,700\ \mathrm{cm}^{-1}$, largely because of the greatly increased complexity and current lack of knowledge of the predissociating $^3\Pi_u$-state manifold at higher energies. For example, as implied in Sec. II B, in order to make further progress towards extending the CSE predissociation model to the levels $b(v>6)$, $c(v>0)$, and $o(v\geqslant 0)$, it will certainly be necessary to consider the Rydberg states, $F\,^3\Pi_u$ and $G\,^3\Pi_u$, together with their interactions. Since there is little known about these states at present, new experimental data would be extremely valuable to help in their characterization. Furthermore, as implied in Sec. III B 2, experimental characterization of the diffuse higher vibrational levels of the $C\,^3\Pi_u$ state would be equally valuable.

Finally, we note that the C and C' potential-energy curves of the current model are not strictly diabatic, in the purely theoretical sense discussed, for example, by Spelsberg and Meyer,[19] since they are dependent on the assumption of R independence for the three couplings $H^{\mathrm{el}}_{CC'}$, H^{so}_{bC}, and $H^{\mathrm{so}}_{bC'}$. This assumption would not necessarily be expected to be valid, especially considering the strong configurational changes in the b and C states as R increases. Nevertheless, the predissociation model clearly works well for the lowest $^1\Pi_u$ levels. However, it remains to be seen whether R-independent couplings will suffice for a correct description of the predissociation of the higher levels. In any case, an *ab initio* study of the $^3\Pi_u$ states of N_2, of similar type to that performed by Spelsberg and Meyer[19] for the $^1\Pi_u$ states, including R-dependent electrostatic interactions, and an R-dependent study of all spin-orbit interactions, would help to clarify this issue. Such a study would be challenging, but

extremely important in enabling the eventual extension of the CSE model to higher energies.

IV. SUMMARY AND CONCLUSIONS

Coupled-channel Schrödinger-equation models of the interacting $^1\Pi_u$ (b,c,o) and $^3\Pi_u$ (C,C') states of N_2 have been combined, through the inclusion of spin-orbit interactions, to produce a five-channel CSE model of the N_2 predissociation. Comparison of the model calculations with an experimental database, consisting principally of detailed new measurements of the vibrational and isotopic dependence of the $^1\Pi_u$ linewidths and lifetimes, provides convincing evidence that the predissociation of the lowest $^1\Pi_u$ levels in N_2 is primarily an indirect process, involving spin-orbit coupling between the $b\,^1\Pi_u$- and $C\,^3\Pi_u$-state levels, the latter of which are themselves heavily predissociated electrostatically by the $C'\,^3\Pi_u$ continuum. The well-known large width of the $b(v=3)$ level in $^{14}N_2$ is caused by an accidental degeneracy with $C(v=9)$. This CSE model provides the first quantitative explanation of the predissociation mechanism for the dipole-accessible $^1\Pi_u$ states of N_2, and is likely to prove useful in the construction of realistic radiative-transfer and photochemical models for nitrogen-rich planetary atmospheres. In order successfully to extend the model to energies higher than $b(v>6)$ at $\sim$105 350 cm^{-1}, further experimental and *ab initio* studies of the $^3\Pi_u$ manifold will likely be necessary.

ACKNOWLEDGMENTS

This paper was initiated during the tenure of H.L-B. as a visiting fellow in the Ultraviolet Physics Unit of the Atomic and Molecular Physics Laboratories at the Australian National University. The authors thank J. P. Sprengers, W. Ubachs, and K.G.H. Baldwin, the authors of the preceding paper in this issue, for providing their results prior to publication, and are particularly grateful to G. Stark (Wellesley College) and K. Yoshino (Harvard-Smithsonian Center for Astrophysics) for their provision of key unpublished data and analyses. This work was partially supported by the Australian Research Council Discovery Program.

[1]H. Lefebvre-Brion, Can. J. Phys. **47**, 541 (1969).
[2]K. Dressler, Can. J. Phys. **47**, 547 (1969).
[3]P. K. Carroll and C. P. Collins, Can. J. Phys. **47**, 563 (1969).
[4]H. Partridge (private communication).
[5]M. Leoni and K. Dressler, Z. Angew. Math. Phys. **22**, 794 (1971).
[6]J. M. Robbe, Ph.D. thesis, University of Lille, 1978.
[7]H. Lefebvre-Brion and R. W. Field, *The Spectra and Dynamics of Diatomic Molecules* (Elsevier, Amsterdam, 2004), pp. 97, 183–190, 310–312, 315–322, 538–542.
[8]W. Ubachs and R. N. Zare, Chem. Phys. **130**, 1 (1989).
[9]H. Helm, I. Hazell, and N. Bjerre, Phys. Rev. A **48**, 2762 (1993).
[10]A. B. van der Kamp, P. C. Cosby, and W. J. van der Zande, Chem. Phys. **184**, 319 (1994).
[11]J. P. Sprengers, W. Ubachs, and K. G. H. Baldwin, J. Chem. Phys. **122**, 144301 (2005), preceding paper.
[12]J. P. Sprengers, W. Ubachs, A. Johansson, A. L'Huillier, C.-G. Wahlström, R. Lang, B. R. Lewis, and S. T. Gibson, J. Chem. Phys. **120**, 8973 (2004).
[13]J. P. Sprengers, A. Johansson, A. L'Huillier, C.-G. Wahlström, B. R. Lewis, and W. Ubachs, Chem. Phys. Lett. **389**, 348 (2004).
[14]G. Stark, K. Yoshino, K. P. Huber, K. Ito, and P. L. Smith, presented as paper M-Po-13 at the 14th International Conference on Vacuum Ultraviolet Radiation Physics, Cairns, 19–23 July, 2004; G. Stark (private communication). Harvard-Smithsonian Center for Astrophysics Molecular Database (http://cfa-www.harvard.edu/amdata/ampdata/N2ARCHIVE/n2home.html).
[15]E. F. van Dishoeck, M. C. van Hemert, A. C. Allison, and A. Dalgarno, J. Chem. Phys. **81**, 5709 (1984).
[16]B. R. Lewis, S. S. Banerjee, and S. T. Gibson, J. Chem. Phys. **102**, 6631 (1995).
[17]P. K. Carroll and R. S. Mulliken, J. Chem. Phys. **43**, 2170 (1965).
[18]D. Stahel, M. Leoni, and K. Dressler, J. Chem. Phys. **79**, 2541 (1983).
[19]D. Spelsberg and W. Meyer, J. Chem. Phys. **115**, 6438 (2001).
[20]W. Ubachs, I. Velchev, and A. de Lange, J. Chem. Phys. **112**, 5711 (2000).
[21]J. P. Sprengers (private communication).
[22]P. F. Levelt and W. Ubachs, Chem. Phys. **163**, 263 (1992).
[23]K. Yoshino (private communication).
[24]J.-Y. Roncin, J.-L. Subtil, and F. Launay, J. Mol. Spectrosc. **188**, 128 (1998).
[25]W. Ubachs, K. S. E. Eikema, and W. Hogervorst, Appl. Phys. B: Photophys. Laser Chem. **57**, 411 (1993).
[26]K. Yoshino, Y. Tanaka, P. K. Carroll, and P. Mitchell, J. Mol. Spectrosc. **54**, 87 (1975).
[27]Y. Kawamoto, M. Fujitake, and N. Ohashi, J. Mol. Spectrosc. **185**, 330 (1997).
[28]J. P. Sprengers, W. Ubachs, K. G. H. Baldwin, B. R. Lewis, and W.-Ü L. Tchang-Brillet, J. Chem. Phys. **119**, 3160 (2003).
[29]There are no Rydberg states of $^1\Sigma_u^-$ symmetry, but effects on the *B*-value database for the *b*-state levels due to rotational perturbation by the $a'\,^1\Sigma_u^-$ valence state cannot be excluded.
[30]The deperturbed difference in energy between $o(v=1)$ and $b(v=9)$ of N_2 is only 6 cm^{-1}, whereas the true difference is 17 cm^{-1}, as can be deduced from Ref. 26.
[31]The potential-energy curves for the Rydberg states *c* and *o* were adjusted smoothly. In the case of the *b* valence state, the inner turning points for the lower levels, the outer turning points for all levels, and the inner-limb extension were allowed to vary freely in the fitting procedure. In particular, this process produced better behavior of the lowest *b*-state levels which lie in the region of the unusually shaped well of the potential.
[32]A. Lofthus and P. H. Krupenie, J. Phys. Chem. Ref. Data **6**, 113 (1977).
[33]J. W. Ledbetter, Jr. and K. Dressler, J. Mol. Spectrosc. **63**, 370 (1976).
[34]J. W. Ledbetter, Jr., J. Chem. Phys. **67**, 3400 (1977).
[35]S. L. Guberman, Geophys. Res. Lett. **18**, 1051 (1991).
[36]S. G. Tilford, J. T. Vanderslice, and P. G. Wilkinson, Astrophys. J. **142**, 1203 (1965).
[37]P. K. Carroll, Proc. R. Soc. London, Ser. A **272**, 270 (1962).
[38]Y. Tanaka and A. S. Jursa, J. Opt. Soc. Am. **51**, 1239 (1961).
[39]H. H. Michels, Adv. Chem. Phys. **45**, 225 (1981).
[40]The *R* values applicable to these computed spin-orbit interactions were not given in Ref. 6.
[41]In Eq. (5), a and ζ are single-electron-molecular and atomic spin-orbit parameters, respectively. The low value results from the molecular parameter depending on the diffuse $3p\pi_u$ Rydberg MO, together with the $1/r_{ij}^3$ dependence inherent in the spin-orbit operator.
[42]A. E. Douglas, Astrophys. J. **117**, 380 (1953).
[43]All *B* values in this work are *effective* values for $J\leqslant 5$. Computed values are determined from separate CSE calculations for $J=0$ and $J=5$.
[44]B. Buijsse, W. J. van der Zande, A. T. J. B. Eppink, D. H. Parker, B. R. Lewis, and S. T. Gibson, J. Chem. Phys. **108**, 7229 (1998).
[45]$H_{CC'}^{el}$ is assumed to be positive.
[46]It should be noted that the *R*-value grid used by Partridge (Ref. 4) is too sparse to allow an accurate determination of the minimum *C*-*C'* separation. Moreover, the spline fitting we have used results in this minimum separation being significantly underestimated in Fig. 1.
[47]The radiative width was assumed to be 0.0014 cm^{-1} FWHM (Ref. 12) for all levels.
[48]T. Hori and T. Endo, Proc. Phys. Math. Soc. Jpn. **23**, 834 (1941).
[49]G. Büttenbender and G. Herzberg, Ann. Phys. **21**, 577 (1935).